ELSEVIER

NeuroImage

www.elsevier.com/locate/ynimg
NeuroImage 27 (2005) 934 – 946

Using voxel-based morphometry to map the structural changes associated with rapid conversion in MCI: A longitudinal MRI study

G. Chételat,[a,*] B. Landeau,[a] F. Eustache,[a,b] F. Mézenge,[a] F. Viader,[a,c] V. de la Sayette,[a,c] B. Desgranges,[a] and J.-C. Baron[d]

[a]*Inserm E0218-Université de Caen, Laboratoire de Neuropsychologie, Centre Cyceron, Bd. H. Becquerel, BP 5229, 14074 Caen cedex, France*
[b]*EPHE, CNRS UMR 8581, Université René Descartes, Paris 5, France*
[c]*Service de Neurologie Vastel, CHU de Caen, France*
[d]*Department of Neurology, University of Cambridge, UK*

Received 5 January 2005; revised 4 May 2005; accepted 6 May 2005
Available online 23 June 2005

Capturing the dynamics of gray matter (GM) atrophy in relation to the conversion from mild cognitive impairment (MCI) to clinically probable Alzheimer's disease (AD) would be of considerable interest. In this prospective study we have used a novel longitudinal voxel-based method to map the progression of GM loss in MCI patients over time and compared converters to non-converters. Eighteen amnestic MCI patients were followed-up for a predefined fixed period of 18 months and conversion was judged according to NINCDS-ADRDA criteria for probable AD. Each patient underwent a high-resolution T1-weighted volume MRI scan both at entry in the study and 18 months later. We used an optimal VBM protocol to compare baseline imaging data of converters to those of non-converters. Moreover, to map GM loss from baseline to follow-up assessment, we used a modified voxel-based morphometry (VBM) procedure specially designed for longitudinal studies. At the end of the follow-up period, seven patients had converted to probable AD. Areas of lower baseline GM value in converters mainly included the hippocampus, parahippocampal cortex, and lingual and fusiform gyri. Regions of significant GM loss over the 18-month follow-up period common to both converters and non-converters included the temporal neocortex, parahippocampal cortex, orbitofrontal and inferior parietal areas, and the left thalamus. However, there was significantly greater GM loss in converters relative to non-converters in the hippocampal area, inferior and middle temporal gyrus, posterior cingulate, and precuneus. This accelerated atrophy may result from both neurofibrillary tangles accumulation and parallel pathological processes such as functional alteration in the posterior cingulate. The ability to longitudinally assess GM changes in MCI offers new perspectives to better understand the pathological processes underlying AD and to monitor the effects of treatment on brain structure.
© 2005 Elsevier Inc. All rights reserved.

Keywords: Alzheimer's disease; Mild cognitive impairment; Longitudinal MRI; Brain mapping; Gray matter loss

Introduction

Capturing the dynamics of gray matter (GM) atrophy in relation to the conversion from mild cognitive impairment (MCI) to clinically probable AD is a crucial goal. As non-invasive surrogate markers of progression to AD are not available, tracking those brain areas that show greatest structural changes over time would be of interest to develop strategies for disease-modifying therapies and to monitor their effects.

Because of its documented high rate of rapid conversion, progressive episodic memory deficit without dementia, termed "amnestic MCI" (Petersen et al., 2001), is well suited to assess the earliest features of AD. Among patients with amnestic MCI, some rapidly convert to AD (to be referred to as "converters" in what follows) whereas others do not, though might do so later ("non-converters"). The most appropriate approach to identify the changes specifically associated with rapid conversion is therefore to compare the changes observed in converters to those observed in non-converters, according to a longitudinal design.

Structural imaging techniques are well suited to assess progression of GM loss. Using longitudinal MRI and each individual's first scan as the reference, changes can be assessed over time against progression to probable AD. However, studies

* Corresponding author. Fax: +33 2 31 47 02 22.
E-mail address: chetelat@cyceron.fr (G. Chételat).
Available online on ScienceDirect (www.sciencedirect.com).

1053-8119/$ - see front matter © 2005 Elsevier Inc. All rights reserved.
doi:10.1016/j.neuroimage.2005.05.015

comparing converters to non-converters have reported discrepant results regarding the rate of temporal lobe atrophy measured with manually traced regions of interest (ROIs), i.e., higher for the hippocampus (Jack et al., 2000, 2004) or for the temporal neocortex (Kaye et al., 1997; Yamada et al., 1996). The ROI method is time consuming, observer dependent, and implies a priori hypotheses regarding the structures to assess, which might explain some of these discrepancies (for a review, see Chételat and Baron, 2003). Furthermore, the ROI method does not allow a comprehensive and objective assessment of the entire cortex and may not be sensitive enough to detect small and more diffuse changes that may arise over a short period of time. Novel automatic methods for computer-assisted image processing offer an attractive alternative (for a review, see Ashburner et al., 2003). These methods have been successfully applied to patients progressing from the moderate to the severe stages of AD (Thompson et al., 2003), and to symptom-free individuals with known autosomal dominant AD mutations (Fox et al., 2001; Scahill et al., 2002). In the present work, we have used voxel-based morphometry (VBM) in sporadic MCI patients to prospectively map the progression of atrophy specifically associated with rapid conversion to AD. From a clinical standpoint, this category of patients clearly represents the main target for therapeutic trials since sporadic AD represents at least 95% of AD cases.

Our purpose in this study was therefore to longitudinally assess the structural changes in amnestic MCI patients using a voxel-based approach. Our primary aim was to compare the progression of GM atrophy over an 18-month period between converters and non-converters so as to identify changes specifically associated with rapid conversion to AD. We made the following hypotheses. Firstly, based on the abovementioned ROI studies, we anticipate a higher rate of atrophy in the hippocampus and the temporal neocortex in converters relative to non-converters. Secondly, based on two voxel-based studies reporting greater atrophy in posterior cingulate, precuneus, and posterior—mainly temporoparietal—association areas in AD relative to MCI (Chételat et al., 2002; Karas et al., 2004), we also predict higher atrophy rates in these posterior areas in relation to the passage from MCI to AD.

Materials and methods

Patients

Eighteen patients with amnestic MCI (Petersen et al., 2001) were prospectively studied. All were exclusively right-handed according to the Edinburgh inventory (Oldfield, 1971), except one patient who scored 67%. They were all recruited through a memory clinic, and all complained of memory impairment. They underwent medical, neurological, neuropsychological, and neuroradiological examinations and were selected according to the following stringent criteria: (i) lack of present or historical evidence of significant neurological, psychiatric, or any other medical disease, use of medication that could affect brain functioning or structure, and depression or substance abuse; (ii) modified Hachinski ischemic score ≤ 2 (Loeb and Gandolfo, 1983); (iii) age over 55 years; (iv) objective memory impairment, as defined by performance 1.5 SD below the normal mean for age-matched controls in at least one subscore of the Grober and Buschke test (Grober and Buschke, 1987) or at the Rey's figure delayed recall test (Rey, 1959); and (v) NINCDS-ADRDA criteria for probable AD (McKhann et al., 1984) not met, as assessed by an extensive neuropsychological examination evidencing normal scores (<1.5 SD below normal mean, adjusted for age and education whenever available) in general intellectual function, i.e., MMSE (Folstein et al., 1975) and Mattis dementia rating scale (Mattis, 1976), and in cognitive functions other than episodic memory, including executive (Stroop test; Golden, 1978), visuospatial (copy of Rey's figure; Rey, 1959), limb praxis (imitation of four meaningless gestures, production of four symbolic gestures and four object utilization gestures), language (writing of 12 irregular words under dictation), and image naming (DO80; Deloche and Hannequin, 1997) functions. Independence in daily living activities was verified during the clinical interviews, and the final decision regarding patient inclusion corresponds to a consensus between the neurologist, the neuropsychologist, and the researcher in charge of the project.

Each patient gave written informed consent to participate in the study, which was approved by the regional ethics committee. All subjects in this study had at least 7 years of education.

Within a few days interval at most from inclusion, each of the 18 MCI patients underwent a high-resolution T1-weighted volume MRI scan. Using the same neuropsychological battery, all subjects were evaluated every 6 months over an 18-month period to assess conversion, i.e., whether they met NINCDS-ADRDA criteria of probable Alzheimer's disease or not. Patients were declared as converters if they had impaired performances (more than 1.5 SD below the normal means according to age and education when available) in at least one of general intellectual function scales as well as in at least two areas of cognition including memory, leading to impaired daily activities as judged by the clinicians from the consultation interviews. Post hoc exclusion criteria included presence of significant neurological, psychiatric or any other medical disease that could affect brain functioning or structure, normal episodic memory performances, or refusal of any follow-up assessment.

A second MRI scan was obtained for each subject at the end of the follow-up period, i.e., 18 months after the first one.

MRI data acquisition

Each subject thus underwent two high-resolution T1-weighted volume MRI scans 18 months apart. Acquisitions consisted of a set of 128 adjacent axial cuts parallel to the anterior commissure–posterior commissure line and with slice thickness 1.5 mm and pixel size 1 × 1 mm, using the SPGR gradient echo sequence (TR = 15.4 s; TE = 3.4 kHz; FOV = 24 cm; matrix = 256 × 256). All the MRI data sets were acquired on the same scanner (1.5 T Signa Advantage echospeed; General Electric) and with the same parameters, by the same team of radiographers, and according to strictly standardized procedures. Standard correction for field inhomogeneities was applied.

MRI data handling and transformations

All image processing steps were carried out using SPM2 and VBM, by the same operators (GC and FM).

Firstly, we compared baseline imaging data of converters to those of non-converters using a standard optimized VBM protocol. The procedure was strictly the same as that described in our previous publication (Chételat et al., 2003a), including customized template creation from the 18 baseline scans, segmentation and normalization of the original (i.e., in native space) baseline scans using these customized priors to determine optimal normalization parameters, application of these optimal parameters to the original baseline scans, and segmentation and smoothing (12 mm) of the normalized data.

Secondly, we assessed GM loss over the 18-month follow-up period using repeated scan measurements. Although standard optimized VBM is adequate and has been validated to map GM loss in various brain disorders using cross-sectional group comparison (Ashburner and Friston, 1997, 2000; Good et al., 2001), including AD (Baron et al., 2001; Karas et al., 2003) and MCI (Chételat et al., 2002, 2003a; Karas et al., 2004; Pennanen et al., 2005), it cannot be used for longitudinal MRI assessments because of potential artefacts due to global changes in brain size over time (see below). We therefore implemented here, with only minor modifications, the VBM procedure specially designed by John Ashburner for longitudinal MRI studies and posted in the SPM mailing-list (http://www.jiscmail.ac.uk/lists/spm.html). This method will be described in detail below. The first part, which is not specific to longitudinal MRI studies, consists in the creation of customized priors for use in the second part, which is the longitudinal VBM procedure per se. For the sake of clarity, a name has been assigned to the resultant image of each step, as indicated in the text and reported in Figs. 1 and 2.

The procedure to create customized templates from specific sample, briefly reported here (see Fig. 1), has been described in detail elsewhere (Good et al., 2001) and already used in our laboratory (Chételat et al., 2003a). A whole brain template was first created from both scans (baseline and follow-up) of each MCI patient (n = 36 scans) by (i) spatially normalizing each original structural MRI scan ('T1_MRI') onto the standard SPM2 T1 template ('T1_SPM2_tpl'), the resultant images being termed 'n_1_MRI'; (ii) creating a mean image ('mean_n_1MRI') from these 36 normalized scans; and (iii) smoothing the resultant mean image with an 8-mm full-width at half-maximum isotropic Gaussian kernel. The resultant whole brain template is termed as 'T1_MCI_tpl' in what follows and in Fig. 1.

Then customized gray matter (GM), white matter (WM), and cerebrospinal fluid (CSF) priors were created by (i) normalizing each original whole brain data set ('T1_MRI') onto the 'T1_MCI_tpl', the resultant images being termed 'n_2_MRI'; (ii) segmenting these normalized data into GM, WM, CSF, and other non-brain partitions, respectively, termed 'GM_n_2MRI', 'WM_n_2MRI', and 'CSF_n_2MRI'; (iii) averaging, for each partition, the 36 normalized images, mean images being termed 'meanGM_n_2MRI', 'meanWM_n_2MRI', and 'meanCSF_n_2MRI'; and (iv) smoothing each partition using a 12-mm full-width at half-maximum kernel. The resultant GM, WM, and CSF customized priors are respectively termed 'GM_MCI_tpl', 'WM_MCI_tpl', and 'CSF_MCI_tpl' in what follows and in Figs. 1 and 2. Note that the customized templates created for the

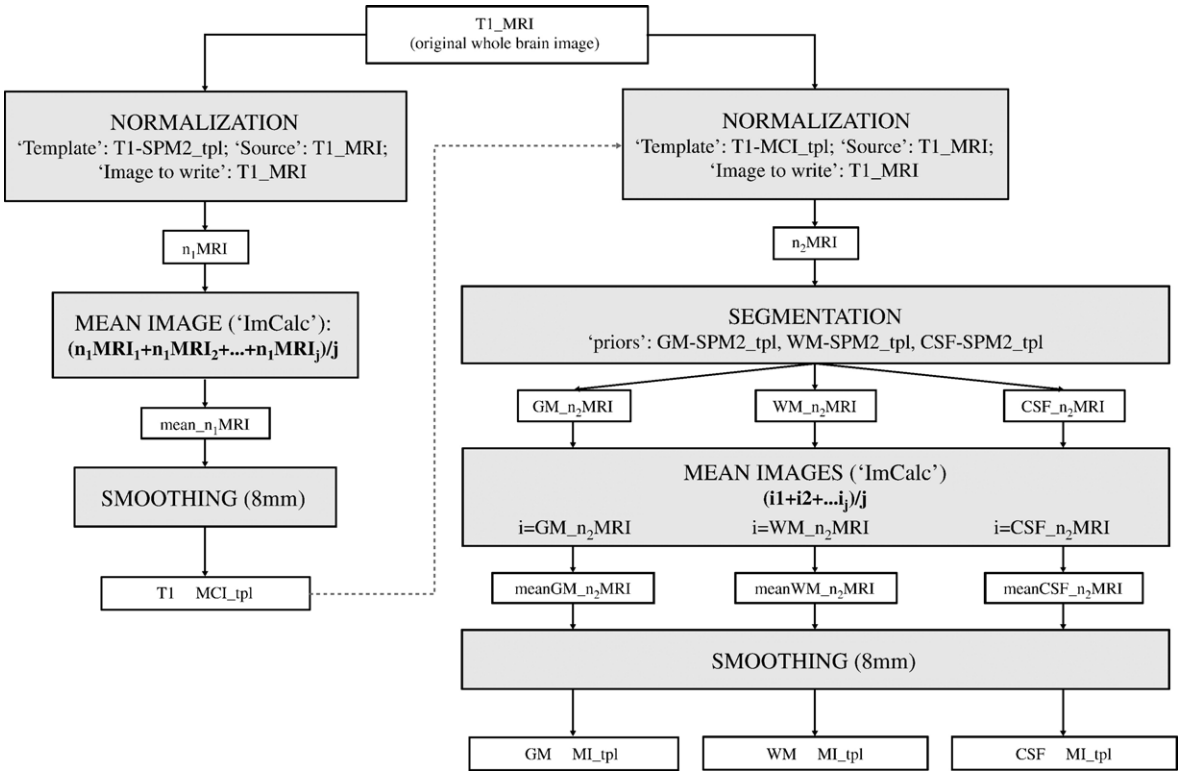

Fig. 1. Procedure used for the creation of customized templates (see Materials and methods for keys and details).

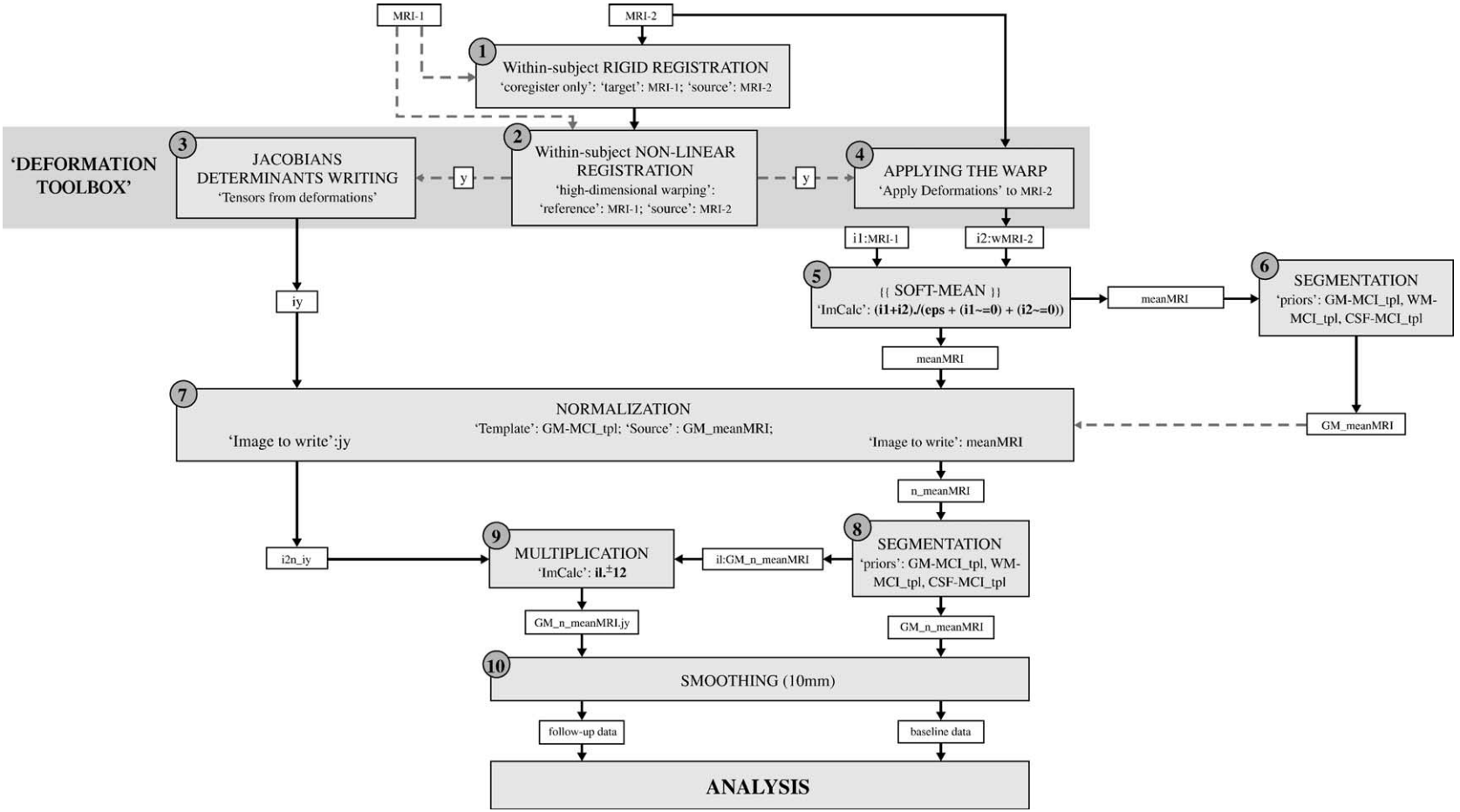

Fig. 2. Procedure used for the longitudinal VBM study (see Materials and methods for keys and details).

longitudinal VBM study are different from those created for the standard VBM study.

The procedure used for the longitudinal VBM study is illustrated in Fig. 2. Succinctly, GM loss is assessed, subject by subject, by transforming the second scan so that it is identical to the first one, the transformation parameters being used to estimate the changes between both scans. More precisely, the method is based on individual high-dimensional warping of the second image ('MRI-2') onto the first image ('MRI-1'). This warping should transform the 'MRI-2' so that it is identical to (or as similar as possible as) the 'MRI-1', the Jacobian determinants ('jy') of the resulting deformation field containing an estimate of the volume changes between both images. Since the warped 'MRI-2' (termed 'wMRI-2') should be equivalent to 'MRI-1', the average of these two images can be used as an estimate of baseline data, and the same image multiplied by the Jacobian determinants as an estimate of follow-up data. To allow group analysis and avoid a cancellation effect of GM loss from WM enlargement, the mean image must be first normalized and then segmented. Modulation is not necessary since the same warp is applied to both images to be compared.

The method consists in the following 10 successive steps (see Fig. 2):

(1) The second scan ('MRI-2') of each subject is rigidly registered onto the first ('MRI-1'), without reslicing (no image is created at this step).
(2) A non-linear registration is performed using high-dimensional warping with 'MRI-1' as the reference image and 'MRI-2' as the source image, the deformation field of the warp being termed 'y'.
(3) The Jacobian determinants of the resulting warp, termed 'jy', are written out.
(4) The deformation field 'y' is applied to 'MRI-2', the resulting image being termed 'wMRI-2'.
(5) 'MRI-1' and 'wMRI-2' are averaged, resulting in a mean image termed 'meanMRI'.
(6) The 'meanMRI' is segmented into GM, WM, CSF, and other non-brain partitions using previously created customized priors (i.e., 'GM_MCI_tpl', 'WM_MCI_tpl', and 'CSF_MCI_tpl'), allowing to use the GM partition, termed 'GM_meanMRI', for the optimal determination of the spatial normalization parameters of the 'meanMRI' and 'jy' data sets.
(7) Parameters from the normalization of the 'GM_meanMRI' onto the previously created 'GM_MCI_tpl' are applied to the 'meanMRI' and 'jy' data sets, resulting in two spatially normalized images respectively termed 'n_meanMRI' and 'n_jy'.
(8) The 'n_meanMRI' is segmented using the 'GM_MCI_tpl', the resultant GM partition being termed 'GM_n_meanMRI'.
(9) The 'GM_n_meanMRI' is multiplied by the 'n_jy', the resultant image being termed 'GM_n_meanMRI.jy'.
(10) Both 'GM_n_meanMRI' and 'GM_n_meanMRI.jy' are smoothed using a 10-mm full-width at half-maximum kernel. The smoothed 'GM_n_meanMRI' is used as an estimate of baseline GM data in analyses, and for the sake of simplicity will be termed 'baseline data' in what follows, while the smoothed 'GM_n_meanMRI.jy', used as an estimate of follow-up GM data in analyses, will be termed 'follow-up data'.

Statistical analysis

For the standard VBM study, a 'compare population: 1 scan/subject (two sample *t* test)' was performed to compare baseline MRI data between converters and non-converters, and the same analysis using baseline age and MMS as nuisance variables was also performed so as to control for the potential effect of these variables.

For the longitudinal VBM study, a 'multi-group: conditions and covariates' analysis was performed within SPM2, with two groups (converters vs. non-converters) and two conditions per subjects (baseline vs. follow-up). Three results were obtained from this analysis.

Firstly, we assessed the within-group GM loss from baseline to follow-up, in both converters and non-converters. To this end, maps of percent annual loss were created for each group, as follows:

$$\text{Percent annual loss map} = \text{Con}/\text{average}(\text{mean\_MRI})*100*12/18;$$

where Con = contrast image (baseline minus follow-up contrast image in converters or in non-converters); average ('mean_MRI') = sum of 'mean_MRI' of all converters or non-converters/number of patients.

Secondly, we assessed the GM loss common to both converters and non-converters, i.e., a conjunction analysis, based on the recently proposed 'valid conjunction inference with the minimum statistic' (Nichols et al., in press). In this test, each comparisons in the conjunction is individually significant, which corresponds to the valid test for a "logical AND".

Finally, we assessed between-group differences to determine brain areas where GM loss is significantly greater in converters than non-converters (i.e., the group × condition interaction).

The reverse contrasts (i.e., follow-up minus baseline and greater GM loss in non-converters than converters) were assessed for the sake of completeness.

In all the above tests (i.e., both the standard and the longitudinal VBM studies), the threshold used was 80% of grand mean. Data were generated at $P < 0.005$ (cluster level; uncorrected) using a cut-off of $P < 0.05$, cluster-level corrected for multiple comparisons. Anatomical localization was according to projection onto the corresponding whole brain customized template. In addition, for the longitudinal study, labels and corresponding percentage of voxels belonging to labelized regions were also obtained for each significant cluster using the aal Toolbox ('cluster labeling'; see Tzourio-Mazoyer et al., 2002), after normalization of the labeled MNI template onto the 'T1_MCI_tpl'.

Results

Clinical data

At completion of the 18-month follow-up period, seven patients were declared as converters, while the remaining 11 patients still had isolated memory deficits (non-converters). The characteristics of both groups are listed in Table 1. They differed neither in mean age nor in mean years of education, but converters scored significantly less at the MMSE than non-converters at entry into the study.

Table 1
Characteristics of the patient samples

	MCI	Converters	Non-converters
Number (women)	18 (11)	7 (4)	11 (7)
Age (years): mean ± SD	69.8 ± 8.1	74.0 ± 4.6	67.1 ± 8.9
Education (years): mean ± SD	9.8 ± 3.4	10.6 ± 4.2	9.4 ± 2.9
Baseline MMSE: mean ± SD	27.3 ± 1.2	26.6 ± 1.0	27.8 ± 1.2[a]
Follow-up (18 months) MMSE: mean ± SD		24.3 ± 5.1	26.9 ± 2.9[a]

[a] Significantly different from converters ($P < 0.05$).

Standard VBM study

The comparison between baseline data of converters and non-converters revealed no significant cluster of higher GM value, and one single cluster of lower GM value, in converters using the $P < 0.05$ (cluster level, corrected) threshold. This cluster extended into the posterior hippocampus, parahippocampal cortex, and lingual and fusiform gyri of the right hemisphere (MNI coordinates of the most significant peak: 16 −62 −14; cluster size $k = 4499$ voxels; P cluster-level corrected = 0.03; see Fig. 3A). For the sake of completeness, we also report here the clusters of lower GM value in converters using a less stringent threshold of $k > 500$ voxels (not surviving the P cluster-level corrected threshold). Clusters were found in the left superior and middle temporal cortex (−65 −28 −5; see Fig. 3B1), left lingual—fusiform—parahippocampal area (−26 −45 −5; see Fig. 3B2), bilateral rectus and orbitofrontal gyri (6 47 −29; see Fig. 3B3), right anterior hippocampus and amygdala (26 −11 −16; see Fig. 3B4), and the right superior temporal gyrus (48 −36 8; see Fig. 3B5).

Finally, introducing baseline age and MMS as nuisance variables, no cluster survived the P cluster-level corrected threshold, but lower GM value in converters was recovered using a less stringent threshold at almost identical location.

Longitudinal VBM study

Fig. 4 illustrates the percent annual GM loss in converters and non-converters. Annual losses ranged from 0% to 4.5% in converters and from 0% to 4% in non-converters. Highest rates (about 2.5–4.5%) concerned the temporal lobe—more specifically the temporal pole, medial temporal region (including the entorhinal cortex), and lateral temporal cortex—cingulate gyrus, and prefrontal cortex in converters, but mainly the latter in non-converters (Fig. 4).

Fig. 5 illustrates the significant gray matter loss in both converters and non-converters (conjunction analysis). Regions of significant loss were essentially symmetrically distributed and more prominently involved the lateral and medial temporal areas (especially the temporal pole, left parahippocampal cortex, and middle and inferior temporal gyri), the orbitofrontal and inferior parietal areas, and the left thalamus. There was no significant cluster when assessing the reverse contrast (follow-up minus baseline).

Over and above this common GM loss, statistically significant regional differences were found between the two groups (Fig. 6 and Table 2). They exclusively consisted in greater GM loss in converters as compared to non-converters, while the reverse contrast revealed no significant cluster. Areas of greater GM loss in converters were essentially symmetrically distributed and concerned the temporal neo-

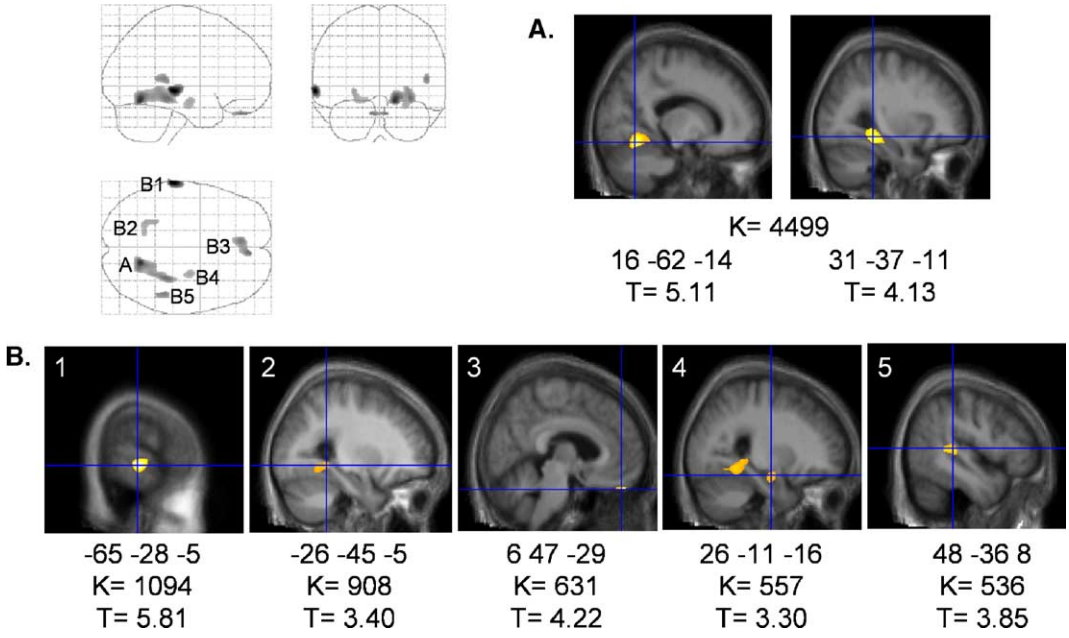

Fig. 3. SPM "glass brain" representation of lower baseline GM value in converters compared to non-converters using a $k > 500$ voxels cut-off, and the superimposition onto sagittal slices of the customized template of the clusters surviving (A), or not surviving (B), the $P < 0.05$ cluster-level corrected threshold. Each cluster (A1–2 and B1–5) is identified onto the superior view of the glass brain.

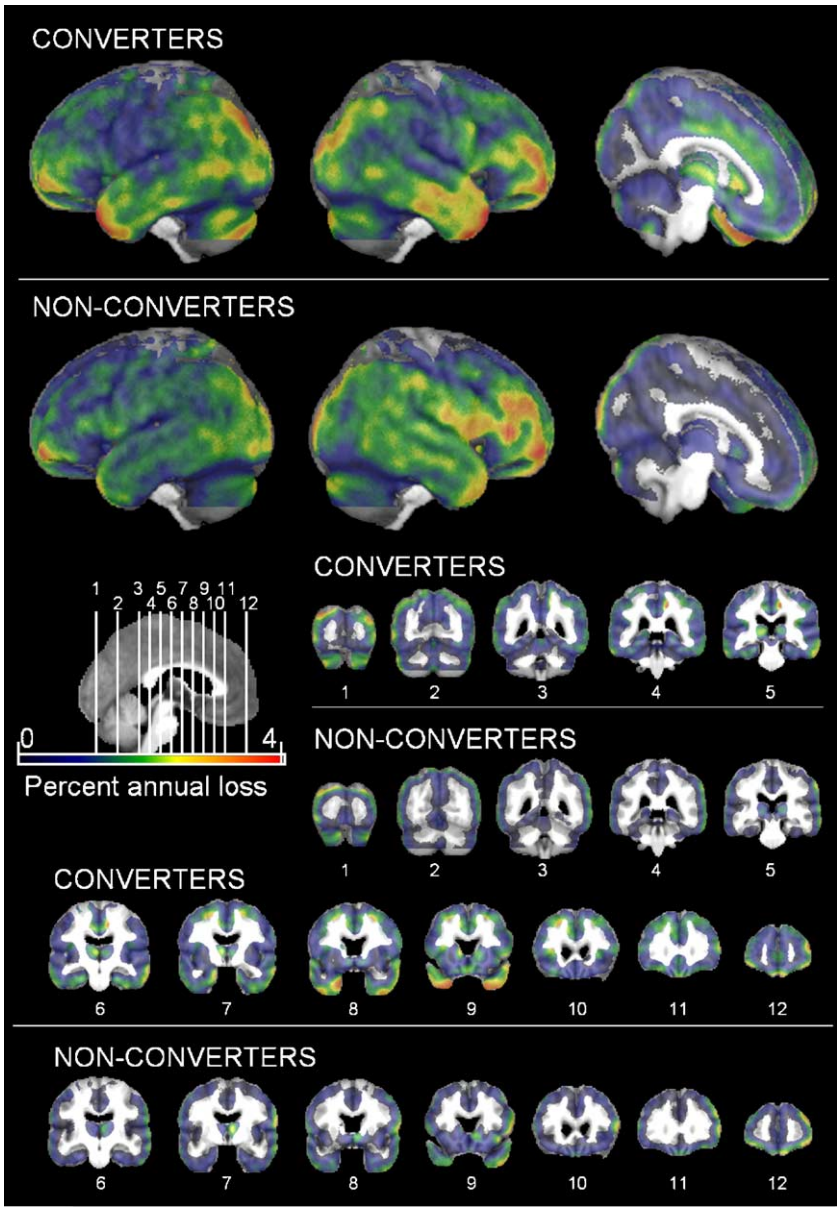

Fig. 4. Percent annual gray matter loss in converters and in non-converters, as projected onto surface rendering from right and left lateral and medial viewpoints (up) and coronal sections (down) of the whole brain customized template (T1_MCI_tpl, see text).

cortex (middle and inferior temporal gyri), hippocampus and parahippocampal area, fusiform gyrus, posterior cingulate gyrus, and precuneus.

Discussion

Methodological considerations

The novel longitudinal voxel-based method implemented here is based on Jacobian determinants estimation from intrasubject high-dimensional warping. This allows one to estimate both baseline and follow-up data from a same mean image of the first scan and the warped second scan. The former corresponds to the mean image itself, and the latter to the mean image multiplied by the Jacobian determinants. This method has the distinct advantage to protect against non-specific subtle differences occurring between the first scan and the warped second scan, or induced by distinct segmentation and spatial normalization steps. Moreover, GM changes are estimated individually, before spatial normalization, thus allowing greater sensitivity. Accordingly, applying this method we found highly focal and substantial GM loss in both groups occurring over an 18-month follow-up period. In an attempt to provide an estimate of the method's sensitivity, we extracted the lowest percent annual loss detected as statistically significant by superimposing the percent annual loss map onto the statistical map thresholded at $P < 0.05$ (cluster-level corrected). Our method was able to detect significant percent annual changes as small as 0.5% in converters and 0.3% in non-converters. Among the factors that contributed to this very good sensitivity, we implemented highly standardized procedures, and all the image processing and analytic steps were performed

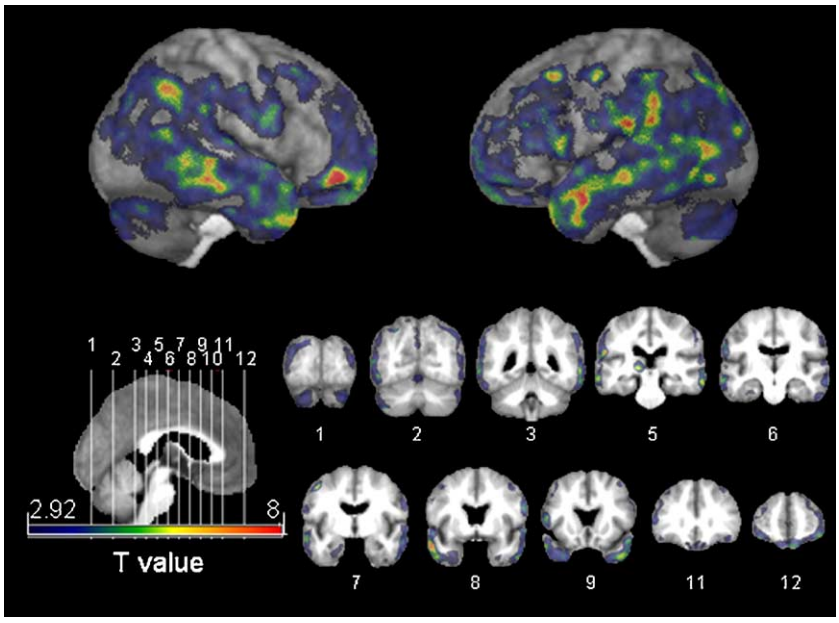

Fig. 5. T-maps of significant ($P < 0.05$, corrected for multiple comparisons) GM loss over the 18-month follow-up period common to both converters and non-converters, as projected onto surface-rendering from right and left lateral viewpoints (up) and coronal sections (down) of the whole brain customized template (T1_MCI_tpl, see text).

by the same two people (GC and FM) throughout the entire duration of this investigation. However, strict quality assurance procedures, including daily phantom acquisitions with 3D measurements and longitudinal evaluations of image distortion, recommended for prospective MRI studies due to the small size of annual changes, were not consistently followed in this study. Thus, the sensitivity of this method would probably have been significantly enhanced had such very tight quality assurance conditions been implemented.

Note that the choice of smoothing parameters is somewhat arbitrary, since there is no strict rule, but depends on scanner resolution and the circumscribed or diffuse nature of the expected effects. For both the standard VBM study and the creation of customized templates (in both the standard and the longitudinal VBM studies), our choice of smoothing was dictated by previous publications (Chételat et al., 2003a; Good et al., 2001). Regarding the smoothing of images used for the longitudinal VBM analysis, we used a 10-mm, instead of the 12-mm, full-width at half-maximum kernel used in the standard VBM because of the longitudinal design of the procedure, where each individual's first scan is used as reference for the follow-up scan. Not surprisingly, results were very similar using filters of 8 or 12 mm instead, with only slight differences in peak significance (data not shown).

Since GM sets are analyzed separately from the CSF, cancellation effects due to CSF enlargement are in principle minimized. However, such effects cannot be completely excluded, notably in the hippocampal region where segmentation is complicated by the interleaving of different tissue classes, as well as by the high degree of expansion of the hippocampal fissure (for example, see Fox et al., 2001). Moreover, smoothing may also induce a contamination of voxel atrophy estimation by surrounding

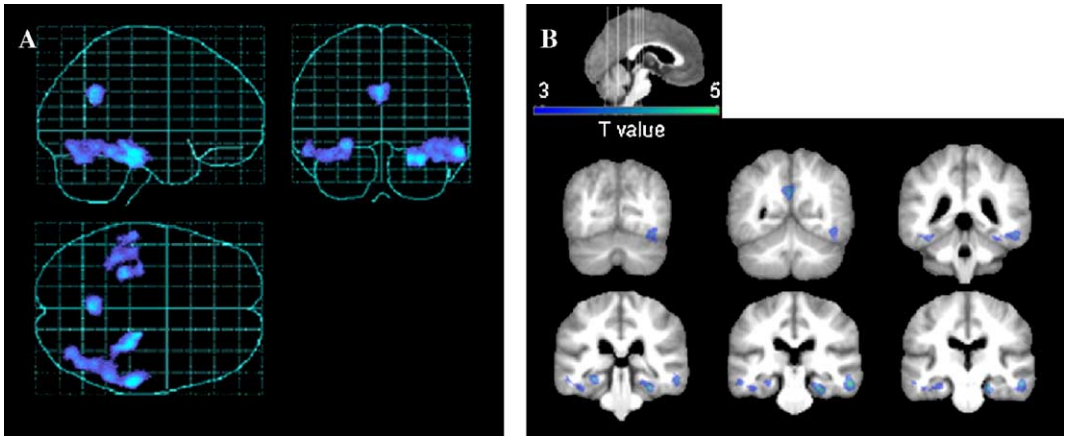

Fig. 6. (A) 'Glass brain' representation showing significant ($P < 0.05$, corrected for multiple comparisons) clusters of greater gray matter loss in converters compared to non-converters. (B) The same results as projected onto coronal sections of the whole brain customized template (T1_MCI_tpl, see text).

Table 2
Location and MNI coordinates of peaks of significantly greater GM loss over the 18-month follow-up period in converters as compared to non-converters

MNI coordinates (mm)			t value	k	$P_{corrected}$ cluster level	Label	%
x	y	z					
59	−25	−19	5.5	7684	<0.001	R inf temporal	34
						R fusiform	24
						R mid temporal	16
						R parahippocampal	13
						R inf occipital	5
−1	−56	31	4.91	1489	0.042	L post cingulate	39
						L precuneus	35
						R precuneus	11
						R post cingulate	8
						R mid cingulate	7
−26	−33	−11	4.54	2972	0.001	L inf temporal	30
						L parahippocampal	26
						L fusiform	23
						L mid temporal	11
						L hippocampus	7

Cluster size is indicated by k = number of voxels in the particular cluster. Label and percentages per cluster were obtained using the aal toolbox (see Materials and methods). Only labels representing more than 5% of the cluster were reported. L = left; R = right; inf = inferior; post = posterior; mid = middle; sup = superior.

voxel values. These effects could have led to some underestimation of hippocampal GM loss. The fact that there was no significant cluster of gray matter expansion over time however indicates that these effects should be marginal only.

In this study, we used a binary approach that consisted in classifying MCI patients as converters or non-converters according to their short-term clinical course (i.e., rapid conversion to AD or not), using criteria used in most current studies. This approach has some limitations since, for instance, MCI patients classified as non-converters might in fact represent slow converters (even though the follow-up period was the same 18 months for all subjects). However, it does have clear clinical relevance, since rapid vs. slow or non-conversion does reflect distinct cognitive evolution, while the identification of rapid converters will be critical in therapeutic studies testing disease-modifying agents.

Finally, we found significant differences between converters and non-converters in baseline MMS, and although not statistically significant, the mean age difference was not negligible (about seven years), unsurprisingly so since age is a major risk factor for AD. Even if small, these differences could in principle influence group comparisons if not controlled. However, the main effects of age and baseline MMS were implicitly modeled as confounds when using the 'multi-group: condition and covariate' design in the longitudinal VBM study. Thus, these variables needed to be explicitly controlled in the standard VBM study only. When assessing GM loss in MCI over 18 months, one observes the superimposition of disease effects upon normal aging processes taking place concomitantly. Since the delay between first and second MRI scans was the same for both groups of patients, aging effects cancelled out when comparing GM loss between converters and non-converters. In contrast, aging processes cannot be dissociated from disease effects in the conjunction analysis and in the percent annual loss map, which is a limitation of this study, our interpretation of age effects being mainly based upon the results of previous publications. Note that this effect should be rather small compared to disease effect, since previous publications reported loss rates below 1% per year in healthy aged subjects (Thompson et al., 2003). Moreover, so as to estimate the effect of aging on GM loss in the present study, we assessed the correlations between age and baseline GM values, and calculated the mean percent annual loss of our MCI sample, in the principal peaks of each significant cluster of the conjunction analysis (see Appendix A). We found significant negative correlations between age and baseline GM values in the left inferior parietal (supramarginal), and left middle frontal gyri and in the left thalamus, with estimated percent annual losses of 0.75%, 0.61%, and 0.51%, respectively.

Clinical data

The relatively high conversion rate (about 26% per year) observed in the present study partly reflects the use of very strict inclusion criteria for MCI patients, i.e., significant and isolated memory deficits both objectively attested by an extensive cognitive evaluation and based on the clinician's consensual judgement from their consultation interview. However, this rate does not take into account the post hoc exclusions of one patient in whom the explicit memory deficit had disappeared at follow-up evaluation, one in whom a brain tumor was diagnosed at follow-up, and one who refused follow-up assessments.

Standard VBM study

To the best of our knowledge, this is the first VBM study comparing baseline MRI data between converters and non-converters. This comparison has been previously assessed in studies using the ROI approach. A significant atrophy of the hippocampal region has been reported in most studies (Convit et al., 2000; Fox et al., 1996; Jack et al., 1999), and the fusiform gyrus (Convit et al., 2000) as well as the superior temporal and anterior cingulate cortex (Killiany et al., 2000) have also been implicated (for a review, see Chételat and Baron, 2003). Our results are consistent with these previous reports, showing at a very stringent cut-off the involvement of a region encompassing the hippocampus, parahippocampal cortex, and lingual and fusiform gyri. Even though not significant using this conservative cluster-level corrected threshold, peaks of atrophy were also present in the superior temporal neocortex, consistent with previous findings using ROIs. Although in general agreement with several lines of evidence, these findings should however be considered with caution in view of their limited statistical validity, which is probably due to the limited sample sizes and the lower sensitivity of VBM when comparing groups made of distinct individuals (in contrast to the longitudinal VBM approach), particularly when controlling for age and MMS which involves a reduction in degrees of freedom.

Main effect of GM loss common to converters and non-converters (conjunction analysis)

Brain sites of most significant GM loss common to converters and non-converters over time included medial and

lateral temporal, inferior parietal and orbitofrontal areas in an almost symmetrical fashion, as well as the left thalamus. This apparent side-to-side brain symmetry of the results is somewhat surprising since many studies point towards an asymmetrical picture in AD, even using a longitudinal whole brain approach. Notably, Thompson et al. (2003) reported faster rates of GM loss in the left hemisphere compared to the right. Although one cannot exclude the presence of asymmetry despite bilateral significance in several areas since we did not formally assess this point, the lack of marked asymmetry could be due to the short inter-scan interval and the intermediate clinical status of the patients.

These findings should reflect normal aging processes as well as potential pathological processes not specifically related to rapid con- version to AD (see above). Previous cross-sectional and longitudinal whole brain studies of normal aging showed most significant gray matter losses in the frontal and parietal (0.38% and 0.55% per year, respectively; Resnick et al., 2003) as compared to the temporal and occipital (0.31% and 0.09%, respectively) lobes (for a review, see Fox and Schott, 2004), with the orbitofrontal and inferior parietal areas being particularly concerned (Resnick et al., 2000, 2003). Our findings regarding the correlation of baseline GM value with age, and our estimate of percent annual loss (see Appendix A), are in good agreement with these previous reports. We also found a less expected effect of age on GM values of the thalamus, a structure rarely assessed in previous longitudinal ROI studies on normal aging, but our finding would merit replication. Thus, in these areas, normal aging processes are thought to account for a significant part of the changes observed in the present study. The GM loss in the temporal lobe may be more specifically associated with the MCI state, possibly reflecting pathological processes present in both converters and non-converters. In support of this interpretation, neuropathological studies (Delacourte et al., 1999) as well as longitudinal MRI studies concur in documenting early and marked alterations in the temporal lobes in subjects at-risk of developing AD, including MCI (Jack et al., 2000; Yamada et al., 1996), very old subjects (Kaye et al., 1997), ApoE4 carriers (Moffat et al., 2000; Mori et al., 2002), and asymptomatic subjects with familial AD (Fox et al., 1996; Schott et al., 2003). Regarding the thalamus, over and above potential age effects, our finding of significant GM loss is consistent with several studies converging toward this structure being morphologically (Chételat et al., 2002; Karas et al., 2004) and functionally (Chételat et al., 2003b; Nestor et al., 2003) affected in MCI. Moreover, the thalamus is implicated in the limbic memory circuit and more particularly has been shown to be associated with episodic memory deficits notably in AD (Desgranges et al., 1998). However, the pathological process underlying this morphological alteration remains unclear since the thalamus is not classically described as an early site of neuropathological alteration. A disconnection mechanism from medial temporal structures has been proposed to account for the early thalamic metabolic deficit, and this functional alteration could have accelerated the atrophy process (for instance, see Nestor et al., 2004).

Distribution of percent annual GM loss

In the present study, the annual rate of GM loss ranged from 0% to 4%, with the highest rates present in frontal, temporal, and cingulate cortices in converters, and in frontal areas in non-converters. These findings are largely consistent with previous longitudinal studies, our rates being intermediate between those reported in normal aging (less than 1% per year; Thompson et al., 2003; Resnick et al., 2003) and those found in AD (5.3 ± 2.3% per year; Thompson et al., 2003). Regarding the hippocampus, we found a 1–2% annual loss while slightly higher changes were found in ROI studies of at-risk populations (2–3% per year; Cardenas et al., 2003; Jack et al., 2000, 2004; Kaye et al., 1997; Schott et al., 2003). This difference may be due to under-estimation of hippocampal GM loss in the present study (see above), but conversely the above studies may have overestimated hippocampal atrophy rates because white matter was included within the ROIs. In contrast, we found areas of marked (~4%) annual GM loss in the temporal neocortex. The above ROI studies generally reported a 1–2% rate in this structure, probably because the whole-region sampling with ROI led to lower estimates. Finally, the annual rates of GM loss found in our study for the entorhinal cortex were particularly marked, in the 3–4% range in converters, a finding in accordance with several previous longitudinal ROIs studies reporting higher volume change in the entorhinal cortex than in the hippocampus (Cardenas et al., 2003; Schott et al., 2003; Jack et al., 2004).

GM loss in converters as compared to non-converters

Comparing progression of GM loss between converters and non-converters revealed highly significant differences in circumscribed areas, suggesting that accelerated pathology specifically takes place in those MCI patients destined to rapidly develop the symptoms that characterize clinically probable AD. As discussed above, these differences can reflect neither an age effect nor initial differences in global cognitive impairment since these variables were implicitly modeled as confounds.

Consistent with our hypothesis, the region-specific differences specifically associated with rapid conversion to AD involved the hippocampal area, inferior and middle temporal neocortex, and posterior cingulate. In previous longitudinal ROI studies, higher rates of volume loss in converters as compared to non-converters concerned the entorhinal cortex and hippocampal structures (Jack et al., 2000, 2004) and the temporal neocortex (Kaye et al., 1997; Yamada et al., 1996). The present study revealed accelerated atrophy in both the medial and the lateral temporal regions, suggesting that our objective voxel-based longitudinal approach has good sensitivity to gray matter changes over time (see also Testa et al., 2004).

Note that there is partial overlap between areas of higher GM loss in converters compared to non-converters, and areas of common loss, notably involving the inferior and middle temporal neocortex. These results indicate that in these areas the atrophy process, though significant in both groups, is differentially faster in converters. Thus, GM loss differences between converters and non-converters are not only qualitative (i.e., involving supplementary areas in converters), but also quantitative. Accordingly, temporal neocortex likely is the target of an on-going atrophic process in MCI, but one that is specifically associated with rapid conversion to AD only when it reaches a critical rate.

Our results are strikingly similar to those reported in longitudinal studies of the familial form of AD, despite the use of an entirely different image processing method (Fox et al., 2001; Scahill et al., 2002). More particularly, Scahill et al. (2002)

reported higher rates of hippocampus and precuneus atrophy in presymptomatic familial AD subjects as compared to healthy controls. In their study however, the temporal neocortex showed accelerated atrophy only in patients who developed clinically probable AD. This discrepancy with our study may stem from several methodological differences, including the longitudinal mapping technique, the sample size, and above all the patients characteristics, since Scahill and colleagues studied asymptomatic individuals with familial AD, whereas we studied sporadic MCI patients both memory impaired and older.

Our hypotheses were also driven by the results of two cross-sectional MRI voxel-based studies comparing MCI to AD patients (Chételat et al., 2002; Karas et al., 2004). Both studies reported higher atrophy in the AD group in the temporal neocortex, cingulate cortex, and parietal association areas, while Karas et al. (2004) also found a significant difference in the hippocampus. Based on these findings, it would follow logically that higher atrophy rates should be present in those same structures in MCI patients that convert to AD. Accordingly, we found higher rates of atrophy in the temporal neocortex, hippocampal region, and posterior cingulate/precuneus in converters compared to non-converters. The lack of significant differences in other posterior association areas does not exclude the possibility that accelerated atrophy in these regions may develop at a later stage of AD (note that in our study the converters had very mild dementia when they were diagnosed with AD; MMSE = 24.3 ± 5.1, see Table 1).

In our study, the highest rates of atrophy were found in the anterior, inferior, middle, and medial parts of the temporal lobes. According to postmortem studies, the MCI stage is characterized by histopathological changes affecting the anterior, inferior, and middle temporal cortex, in addition to the hippocampal area which is already involved in healthy aging (Delacourte et al., 1999). In contrast, the superior temporal cortex becomes involved, together with the anterior frontal and inferior parietal cortices, at a later stage only, when patients become demented. This parallel evolution between the neuropathological changes described in postmortem studies and the rates of atrophy reported here suggests a direct link between these two processes, a kind of cascade whereby the presence of neurofibrillary tangles would accelerate GM loss.

Although the posterior cingulate cortex has not been described as the earliest site of NFT accumulation, it is the earliest and most prominent area of metabolic decrement in AD relative to age-matched controls, even present at a predementia stage potentially as the result of functional disconnection from the hippocampal region (Chételat et al., 2003b; Johnson et al., 2001; Meguro et al., 1999; Minoshima et al., 1997; Nestor et al., 2003, 2004; Small et al., 2000). One could therefore argue that, in the posterior cingulate cortex, the early metabolic impairment might induce greater atrophy rates in the following 18 months observed in the present study. As significant GM loss has been reported in this structure in MCI relative to controls (Chételat et al., 2002), this might be an early process.

To sum-up, a novel longitudinal voxel-based method, fully automated and implemented in SPM, allowed us to map structural changes over time, both statistically and quantitatively. GM loss was detectable over an 18-month follow-up period in patients with MCI. Greatest changes occurred in the temporal lobe and the posterior cingulate in those patients who fulfilled clinically probable AD criteria over this period. This accelerated atrophy may occur as a result of neurofibrillary tangles accumulation but may also be induced by parallel pathological processes, such as functional disruption. Future research focusing on the relationships between GM loss acceleration on one hand, and neuropathological, metabolic, and cognitive alterations on the other, may help to address this issue. To be able to longitudinally assess GM changes offers new perspectives to better understand the pathological processes underlying AD and to monitor the effects of new treatments on brain structure.

Acknowledgments

We are indebted to Ms. C. Lalevée, Ms. A. Pélerin, D. Hannequin, and B. Dupuy for their help in this study. This work was supported by INSERM U.320, Ministère de la Santé (PHRC, Principal Investigator: J-C Baron), Ministère de l'éducation nationale, Fondation France-Alzheimer and Institut de Recherches Internationales Servier.

Appendix A

Results of the correlations between age and baseline GM values in the principal peaks of each significant cluster of the conjunction analysis (MNI coordinates, localization, *P* value, correlation coefficient = *r*, slope (in percentage), and mean percent annual loss (PAL) estimation from the simple linear regression equation using the mean age of the sample).

MNI (*x y z*)	Localization (Brodmann area)	*P* value	*r*	% slope	PAL
46 47 −13	R orbitofrontal G (11)	0.824	0.056	0.030	0.072
−54 1 −25	L middle temporal G (21)	0.084	0.42	0.141	0.236
−53 −27 21	L inferior parietal/supramarginal G (40)	0.001*	−0.695	−0.422	−0.747
67 −33 −14	R middle temporal G (21)	0.390	−0.216	−0.089	−0.143
55 −58 42	R inferior parietal/supramarginal G (40)	0.506	−0.168	−0.068	−0.131
−52 −74 6	Left middle occipital G (19)	0.466	−0.183	−0.074	−0.180
−37 21 50	L middle frontal G (6/8)	0.047*	−0.474	−0.253	−0.610
−11 −30 0	L thalamus	0.048*	−0.472	−0.318	−0.506
−42 −7 51	L precentral G (4)	0.849	−0.048	−0.021	−0.042
4 −55 −7	Vermis	0.837	−0.052	−0.031	−0.050

G = gyrus; L = left; R = right; *$P < 0.05$.

References

Ashburner, J., Friston, K., 1997. Multimodal image coregistration and partitioning—A unified framework. NeuroImage 6, 209–217.

Ashburner, J., Friston, K.J., 2000. Voxel-based morphometry—The methods. NeuroImage 11, 805–821.

Ashburner, J., Csernansky, J.G., Davatzikos, C., Fox, N.C., Frisoni, G.B., Thompson, P.M., 2003. Computer-assisted imaging to assess brain structure in healthy and diseased brains. Lancet Neurol. 2, 79–88.

Baron, J.C., Chételat, G., Desgranges, B., Perchey, G., Landeau, B., de la Sayette, V., Eustache, F., 2001. In vivo mapping of gray matter loss with voxel-based morphometry in mild Alzheimer's disease. NeuroImage 14, 298–309.

Cardenas, V.A., Du, A.T., Hardin, D., Ezekiel, F., Weber, P., Jagust, W.J., Chui, H.C., Schuff, N., Weiner, M.W., 2003. Comparison of methods for measuring longitudinal brain change in cognitive impairment and dementia. Neurobiol. Aging 24, 537–544.

Chételat, G., Baron, J.C., 2003. Early diagnosis of Alzheimer's disease: contribution of structural neuroimaging. NeuroImage 18, 525–541.

Chételat, G., Desgranges, B., de la Sayette, V., Viader, F., Eustache, F., Baron, J.C., 2002. Mapping gray matter loss with voxel-based morphometry in mild cognitive impairment. NeuroReport 13, 1939–1943.

Chételat, G., Desgranges, B., de la Sayette, V., Viader, F., Berkouk, K., Landeau, B., Lalevée, C., Le Doze, F., Dupuy, B., Hannequin, D., Baron, J.C., Eustache, F., 2003a. Dissociating atrophy and hypometabolism impact on episodic memory in mild cognitive impairment. Brain 126, 1955–1967.

Chételat, G., Desgranges, B., de la Sayette, V., Viader, F., Eustache, F., Baron, J.C., 2003b. Mild cognitive impairment: can FDG-PET predict who is to rapidly convert to Alzheimer's disease? Neurology 60, 1374–1377.

Convit, A., de Asis, J., De Leon, M.J., Tarshish, C.Y., De Santi, S., Rusinek, H., 2000. Atrophy of the medial occipitotemporal, inferior, and middle temporal gyri in non-demented elderly predict decline to Alzheimer's disease. Neurobiol. Aging 21, 19–26.

Delacourte, A., David, J.P., Sergeant, N., Buée, L., Wattez, A., Vermersch, P., Ghozali, F., Fallet-Bianco, C., Pasquier, F., Lebert, F., Petit, H., Di Menza, C., 1999. The biochemical pathway of neurofibrillary degeneration in aging and Alzheimer's disease. Neurology 52, 1158–1165.

Deloche, G., Hannequin, D., 1997. Test De Dénomination Orale d'images DO80. Française, Paris.

Desgranges, B., Baron, J.C., de la Sayette, V., Petit-Taboue, M.C., Benali, K., Landeau, B., Lechevalier, B., Eustache, F., 1998. The neural substrates of memory systems impairment in Alzheimer's disease. A PET study of resting brain glucose utilization. Brain 121, 611–631.

Folstein, M.F., Folstein, S.E., McHugh, P.R., 1975. "Mini-mental state." A practical method for grading the cognitive state of patients for the clinician. J. Psychiatr. Res. 12, 189–198.

Fox, N.C., Schott, J.M., 2004. Imaging cerebral atrophy: normal ageing to Alzheimer's disease. Lancet 363, 392–394.

Fox, N.C., Warrington, E.K., Freeborough, P.A., Hartikainen, P., Kennedy, A.M., Stevens, J.M., Rossor, M.N., 1996. Presymptomatic hippocampal atrophy in Alzheimer's disease, a longitudinal MRI study. Brain 119, 2001–2007.

Fox, N.C., Crum, W.R., Scahill, R.I., Stevens, J.M., Janssen, J.C., Rossor, M.N., 2001. Imaging of onset and progression of Alzheimer's disease with voxel-compression mapping of serial magnetic resonance images. Lancet 358, 201–205.

Golden, C.J., 1978. The Stroop Color and Word Test: A manual for Clinical and Experimental Uses. Chicago, Stoelting.

Good, C.D., Johnsrude, I.S., Ashburner, J., Henson, R.N., Friston, K.J., Frackowiak, R.S., 2001. A voxel-based morphometric study of ageing in 465 normal adult human brains. NeuroImage 14, 21–36.

Grober, E., Buschke, H., 1987. Genuine memory deficits in dementia. Dev. Neuropsychol. 3, 13–36.

Jack, C.R., Petersen, R.C., Xu, Y.C., O'Brien, P.C., Smith, G.E., Ivnik, R.J., Boeve, B.F., Waring, S.C., Tangalos, E.G., Kokmen, E., 1999. Prediction of AD with MRI-based hippocampal volume in mild cognitive impairment. Neurology 52, 1397–1403.

Jack, C.R., Petersen, R.C., Xu, Y., O'Brien, P.C., Smith, G.E., Ivnik, R.J., Boeve, B.F., Tangalos, E.G., Kokmen, E., 2000. Rates of hippocampal atrophy correlate with change in clinical status in aging and AD. Neurology 55, 484–489.

Jack Jr., C.R., Shiung, M.M., Gunter, J.L., O'Brien, P.C., Weigand, S.D., Knopman, D.S., Boeve, B.F., Ivnik, R.J., Smith, G.E., Cha, R.H., Tangalos, E.G., Petersen, R.C., 2004. Comparison of different MRI brain atrophy rate measures with clinical disease progression in AD. Neurology 62, 591–600.

Johnson, K.A., Lopera, F., Jones, K., Becker, A., Sperling, R., Hilson, J., Londono, J., Siegert, I., Arcos, M., Moreno, S., Madrigal, L., Ossa, J., Pineda, N., Ardila, A., Roselli, M., Albert, M.S., Kosik, K.S., Rios, A., 2001. Presenilin-1-associated abnormalities in regional cerebral perfusion. Neurology 56, 1545–1551.

Karas, G.B., Burton, E.J., Rombouts, S.A., van Schijndel, R.A., O'Brien, J.T., Scheltens, P., McKeith, I.G., Williams, D., Ballard, C., Barkhof, F., 2003. A comprehensive study of gray matter loss in patients with Alzheimer's disease using optimized voxel-based morphometry. NeuroImage 18, 895–907.

Karas, G.B., Scheltens, P., Rombouts, S.A., Visser, P.J., van Schijndel, R.A., Fox, N.C., Barkhof, F., 2004. Global and local gray matter loss in mild cognitive impairment and Alzheimer's disease. NeuroImage 23, 708–716.

Kaye, J.A., Swihart, T., Howieson, D., Dame, A., Moore, M.M., Karnos, T., Camicioli, R., Ball, M., Oken, B., Sexton, G., 1997. Volume loss of the hippocampus and temporal lobe in the healthy elderly persons destined to develop dementia. Am. Acad. Neurol. 48, 1297–1304.

Killiany, R.J., Gomez-Isla, T., Moss, M., Kikinis, R., Sandor, T., Jolesz, F., Tanzi, R., Jones, K., Hyman, B.T., Albert, M.S., 2000. Use of structural magnetic resonance imaging to predict who will get Alzheimer's disease. Ann. Neurol. 47, 430–439.

Loeb, C., Gandolfo, C., 1983. Diagnostic evaluation of degenerative and vascular dementia. Stroke 14, 399–401.

McKhann, G., Drachman, D., Folstein, M., Katzman, R., Price, D., Stadlan, E.M., 1984. Clinical diagnosis of Alzheimer's disease: report of the NINCDS-ADRDA Work Group under the auspices of Department of Health and Human Services Task Force on Alzheimer's Disease. Neurology 34, 939–944.

Meguro, K., Blaizot, X., Kondoh, Y., Le Mestric, C., Baron, J.C., Chavoix, C., 1999. Neocortical and hippocampal glucose hypometabolism following neurotoxic lesions of the entorhinal and perirhinal cortices in the non-human primate as shown by PET. Implications for Alzheimer's disease. Brain 122, 1519–1531.

Minoshima, S., Giordani, B., Berent, S., Frey, K.A., Foster, N.L., Kuhl, D.E., 1997. Metabolic reduction in the posterior cingulate cortex in very early Alzheimer's disease. Ann. Neurol. 42, 85–94.

Moffat, S.D., Szekely, C.A., Zonderman, A.B., Kabani, N.J., Resnick, S.M., 2000. Longitudinal change in hippocampal volume as a function of apolipoprotein E genotype. Neurology 55, 134–136.

Mori, E., Lee, K., Yasuda, M., Hashimoto, M., Kazui, H., Hirono, N., Matsui, M., 2002. Accelerated hippocampal atrophy in Alzheimer's disease with apolipoprotein E epsilon4 allele. Ann. Neurol. 51, 209–214.

Nestor, P.J., Fryer, T.D., Ikeda, M., Hodges, J.R., 2003. Retrosplenial cortex (BA 29/30) hypometabolism in mild cognitive impairment (prodromal Alzheimer's disease). Eur. J. Neurosci. 18, 2663–2667.

Nestor, P.J., Scheltens, P., Hodges, J.R., 2004. Advances in the early detection of Alzheimer's disease. Nat. Rev., Neurosci. 5, S34–S41 (Suppl.).

Nichols, T., Brett, M., Andersson, J., Wager, T., Poline, J.B., 2005. Valid conjunction inference with the minimum statistic. NeuroImage 25 (3) (Apr 15), 653–660.

Oldfield, R.C., 1971. The assessment and analysis of handedness: the Edinburgh inventory. Neuropsychologia 9, 97–113.

Pennanen, C., Testa, C., Laakso, M.P., Hallikainen, M., Helkala, E.L., Hanninen, T., Kivipelto, M., Kononen, M., Nissinen, A., Tervo, S., Vanhanen, M., Vanninen, R., Frisoni, G.B., Soininen, H., 2005. Voxel based morphometry study on mild cognitive impairment. J. Neurol., Neurosurg. Psychiatry 76, 11–14.

Petersen, R.C., Doody, R., Kurz, A., Mohs, R.C., Morris, J.C., Rabins, P.V., Ritchie, K., Rossor, M., Thal, L., Winblad, B., 2001. Current concepts in mild cognitive impairment. Arch. Neurol. 58, 1985–1992.

Resnick, S.M., Goldszal, A.F., Davatzikos, C., Golski, S., Kraut, M.A., Metter, E.J., Bryan, R.N., Zonderman, A.B., 2000. One-year age changes in MRI brain volumes in older adults. Cereb. Cortex 10, 464–472.

Resnick, S.M., Pham, D.L., Kraut, M.A., Zonderman, A.B., Davatzikos, C., 2003. Longitudinal magnetic resonance imaging studies of older adults: a shrinking brain. J. Neurosci. 23, 3295–3301.

Rey, A., 1959. Test de Copie d'Une Figure Complexe de A.Rey. In: Française (Ed.). Paris.

Scahill, R.I., Schott, J.M., Stevens, J.M., Rossor, M.N., Fox, N.C., 2002. Mapping the evolution of regional atrophy in Alzheimer's disease: unbiased analysis of fluid-registered serial MRI. Proc. Natl. Acad. Sci. U. S. A. 99, 4703–4707.

Schott, J.M., Fox, N.C., Frost, C., Scahill, R.I., Janssen, J.C., Chan, D., Jenkins, R., Rossor, M.N., 2003. Assessing the onset of structural change in familial Alzheimer's disease. Ann. Neurol. 53, 181–188.

Small, G.W., Ercoli, L.M., Silverman, D.H., Huang, S.C., Komo, S., Bookheimer, S.Y., Lavretsky, H., Miller, K., Siddarth, P., Rasgon, N.L., Mazziotta, J.C., Saxena, S., Wu, H.M., Mega, M.S., Cummings, J.L., Saunders, A.M., Pericak-Vance, M.A., Roses, A.D., Barrio, J.R., Phelps, M.E., 2000. Cerebral metabolic and cognitive decline in persons at genetic risk for Alzheimer's disease. Proc. Natl. Acad. Sci. U. S. A. 97, 6037–6042.

Testa, C., Laakso, M.P., Sabattoli, F., Rossi, R., Beltramello, A., Soininen, H., Frisoni, G.B., 2004. A comparison between the accuracy of voxel-based morphometry and hippocampal volumetry in Alzheimer's disease. J. Magn. Reson. Imaging 19, 274–282.

Thompson, P.M., Hayashi, K.M., de Zubicaray, G., Janke, A.L., Rose, S.E., Semple, J., Herman, D., Hong, M.S., Dittmer, S.S., Doddrell, D.M., Toga, A.W., 2003. Dynamics of gray matter loss in Alzheimer's disease. J. Neurosci. 23, 994–1005.

Tzourio-Mazoyer, N., Landeau, B., Papathanassiou, D., Crivello, F., Etard, O., Delcroix, N., Mazoyer, B., Joliot, M., 2002. Automated anatomical labeling of activations in SPM using a macroscopic anatomical parcellation of the MNI MRI single-subject brain. NeuroImage 15, 273–289.

Yamada, N., Tanabe, H., Kazui, H., Ikeda, M., Hashimoto, M., Nakagawa, Y., Wada, Y., Okuda, J.I., 1996. Longitudinal neuropsychological and quantitative MRI assessments in early Alzheimer's disease. Alzheimer's Res. 2, 29–36.